Journal of Alloys and Compounds 678 (2016) 439–443

Contents lists available at ScienceDirect

Journal of Alloys and Compounds

journal homepage: http://www.elsevier.com/locate/jalcom

Electronic structure and optical property studies of wurtzite $AgInS_2$ doped by tin

Jianbo Yin [a, b, *], Xuefeng Lu [b], Qizheng Dong [b]

[a] State Key Laboratory of Advanced Processing and Recycling of Non–ferrous Metals, Lanzhou University of Technology, Lanzhou, 730050, China
[b] Key Laboratory of Nonferrous Metal Alloys and Processing, Ministry of Education, Lanzhou University of Technology, Lanzhou 730050, China

ARTICLE INFO

Article history:
Received 10 December 2015
Received in revised form
31 March 2016
Accepted 2 April 2016
Available online 5 April 2016

Keywords:
Metal
Doping
Sulfides

ABSTRACT

The electronic structure and optical property of wurtzite $AgInS_2$ with vacancy defects and tin doping have been investigated by the first principle based on density functional theory. The results show that the intrinsic silver and indium vacancy may lead to the narrowing of bandgap. It shows metal characteristic after a silver atom and an indium atom are respectively replaced by tin atoms in the supercell of wurtzite $AgInS_2$. The optical property study indicates that the absorption curves and reflectivity curves of $AgInS_2$ are blue shift and weakened owing to the existence of vacancy defects and tin doping.

1. Introduction

As a I–III–VI ternary metal compound, $AgInS_2$ is widely used in the fields of photovoltaic cells, photocatalysis, optoelectronics and nonlinear optics due to its excellent optical property and environmentally benign nature [1–3]. In general, $AgInS_2$ crystals have two different polymorphs: chalcopyrite phase and orthorhombic wurtzite phase. The latter has shown more excellent photoelectrical and optical property than that of chalcopyrite, and it has attracted much concentration [4,5]. The experiments and simulated calculations of pure orthorhombic wurtzite $AgInS_2$ indicated that it was a direct bandgap semiconductor with a proper range of light absorption [6,7]. Yet, due to the optical property of pure orthorhombic wurtzite $AgInS_2$ has encountered development limitations, researchers have adopted various routes to improve the property. Metal ion doping is the most effective way to improve optical property of orthorhombic wurtzite $AgInS_2$ for the introduction of impurity levels can improve the bandgap effectively, and it has been found by experiments in recent year that tin doped $AgInS_2$ has very excellent optical property due to the adjustable band gap in the visible region [8–10]. Therefore, it is necessary to study the optical principle of $AgInS_2$ doped by tin via simulated calculation, and it can also offer a valuable proposal for the experiment researchers of $AgInS_2$ study.

The first principle can be used to calculate the band gap and optical property of a semiconductor [11–13]. It has been widely used in optical material calculation to explain the results of experiment of optical materials [14,15]. Doping calculation of a semiconductor is an important application of the first principle, and it has been reported by more and more papers [16–18]. For example, Zhang and his partners calculated hydrogen absorption of the graphene oxide doped by Mg via the first principle calculation [19]; Caliskan and Guner calculated the spin dependent electronic behavior of ZnO doped by Co via the first principle study [20]; Li and his coworkers studied the energy band structure of $BiPO_4$ doped by N via the first principle [21].

In this work, the first principle is adopted to study the electronic structure and optical property of $AgInS_2$ doped by tin, and the purpose is to carry out a theory study of $AgInS_2$ with different structural defects and offer a proposal for the researchers of experiment.

2. Computational details

The first principle calculation of $AgInS_2$ was carried out with the Cambridge Serial Total Energy Package module (CASTP) of material studio 6.0 version. The calculation adopted the supercell of wurtzite $AgInS_2$, which consisted 32 atoms. The core electrons were

* Corresponding author. State Key Laboratory of Advanced Processing and Recycling of Non–ferrous Metals, Lanzhou University of Technology, Lanzhou, 730050, China.
E-mail address: jianbery@163.com (J. Yin).

http://dx.doi.org/10.1016/j.jallcom.2016.04.022
0925-8388/

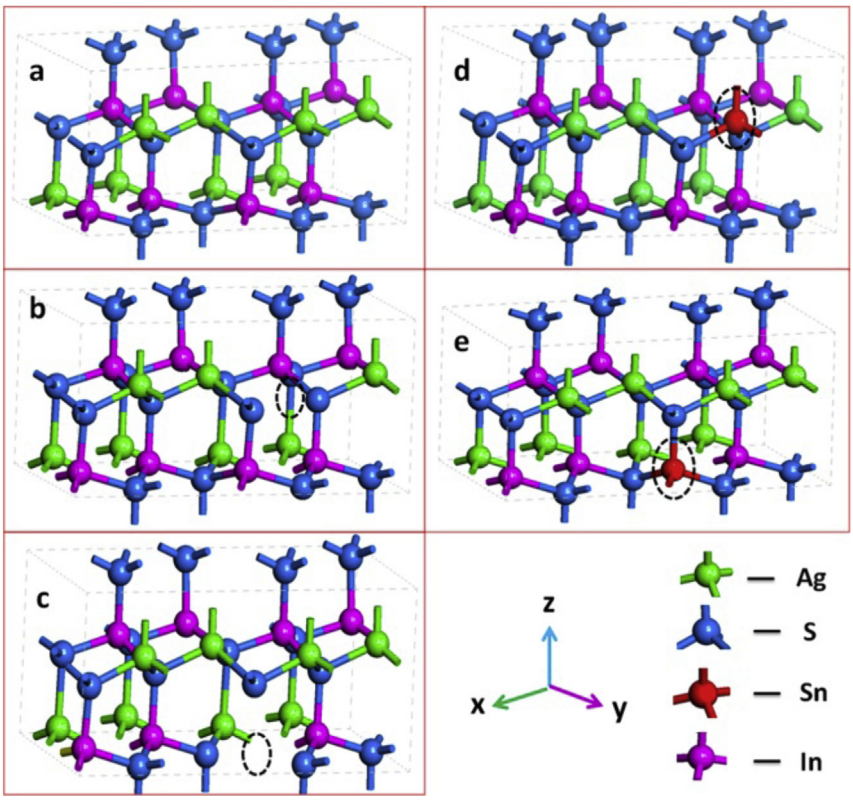

Fig. 1. The supercell crystal structure models of wurtzite $AgInS_2$ with different structural defects. (a) The supercell crystal structure models of pure wurtzite $AgInS_2$; (b) The supercell crystal structure models of wurtzite $AgInS_2$ with silver vacancy; (c) The supercell crystal structure models of wurtzite $AgInS_2$ with indium vacancy; (d) The supercell structure models of wurtzite $AgInS_2$ a silver atom of which is replaced by a tin atom; (e) The supercell structure models of wurtzite $AgInS_2$ an indium atom of which is replaced by a tin atom.

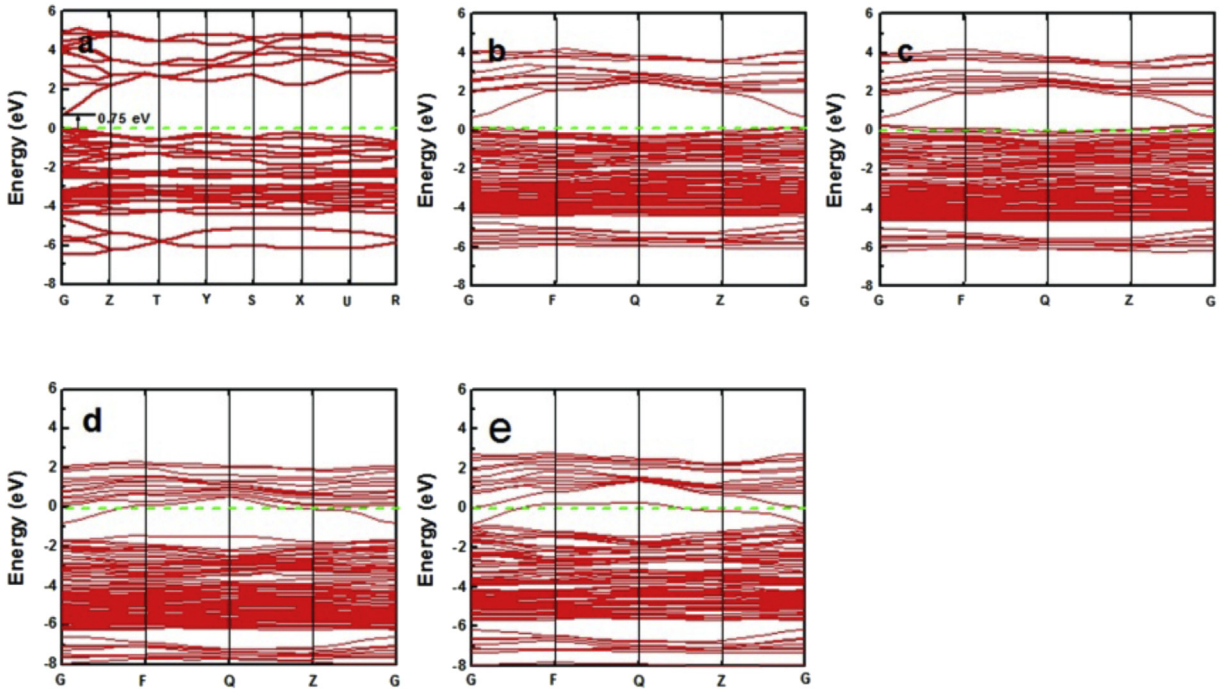

Fig. 2. Band structure of wurtzite $AgInS_2$ with different structural defects. (a) Band structure of pure wurtzite $AgInS_2$; (b) Band structure of wurtzite $AgInS_2$ with silver vacancy; (c) Band structure of wurtzite $AgInS_2$ with indium vacancy; (d) Band structure of wurtzite $AgInS_2$ a silver atom of which is replaced by a tin atom; (e) Band structure of wurtzite $AgInS_2$ an indium atom of which is replaced by a tin atom.

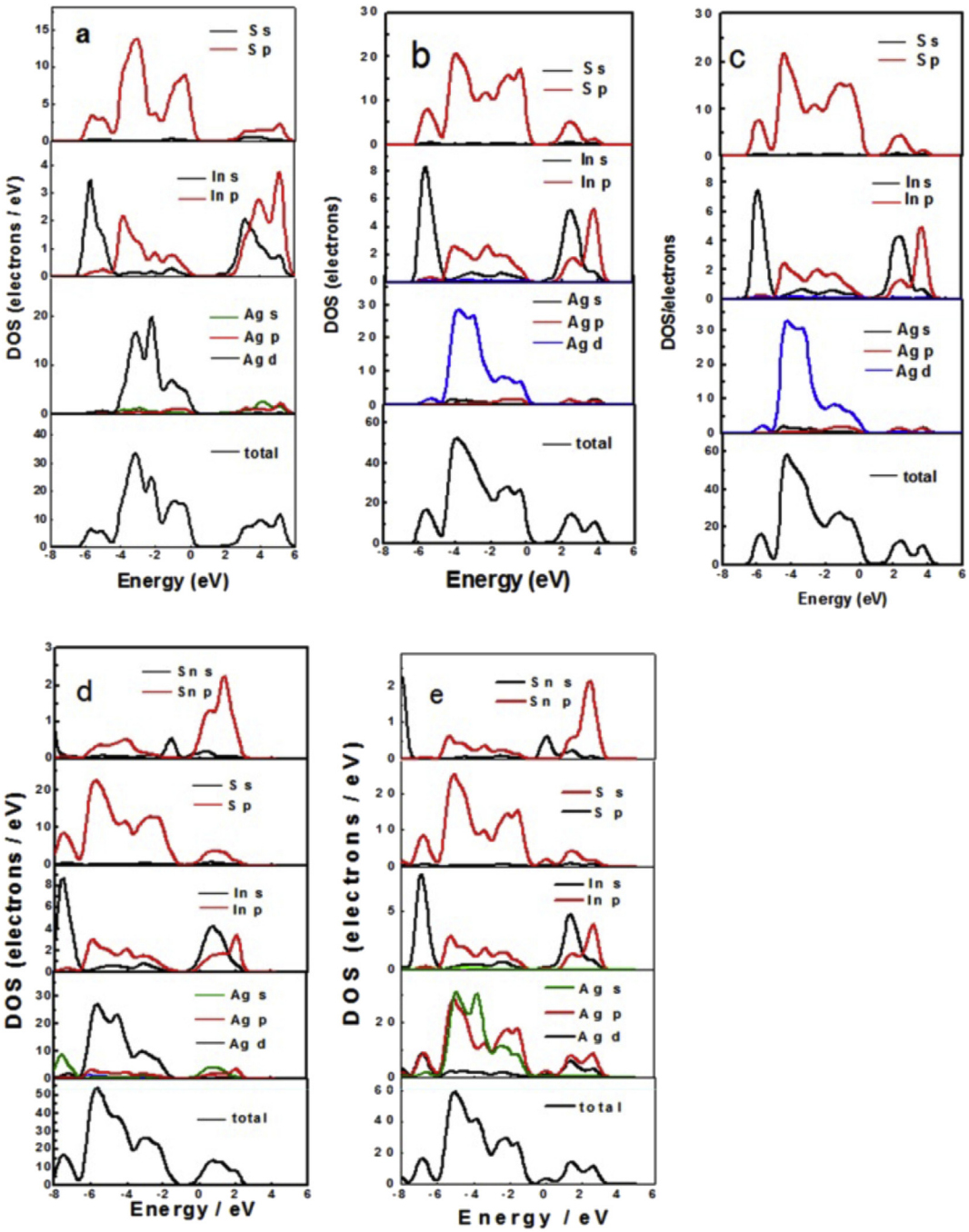

Fig. 3. Density of state of wurtzite $AgInS_2$ with different structural defects. (a) Density of state of pure wurtzite $AgInS_2$; (b) Density of state of wurtzite $AgInS_2$ with silver vacancy; (c) Density of state of wurtzite $AgInS_2$ with indium vacancy; (d) Density of state of wurtzite $AgInS_2$ a silver atom of which is replaced by a tin atom; (e) Density of state of wurtzite $AgInS_2$ an indium atom of which is replaced by a tin atom.

optimized by the Perdew–Burke–Ernzerhof (PBE) of generalized gradient approximation (GGA) functional. And PBE method was used as the exchange–correlation effects of valence electrons. The energy cutoff was chosen 720 eV. The Monkhorst–Pack scheme k-points grid sampling was set as $3 \times 3 \times 4$ for the irreducible Brillouin zone. The electronic configurations are $4s^2 4p^6 4d^{10} 5s^1$ for silver, $5s^2 5p^1$ for indium, $3s^2 3p^4$ for sulfur and $5s^2 5p^2$ for tin.

3. Results and discussions

The space group of wurtzite $AgInS_2$ is $Pna2_1$ and the local symmetry is c_{2v}^9. The phase structure of $AgInS_2$ is chosen wurtzite orthorhombic structure which is still stable at high temperature [22]. The calculation adopts the supercell of wurtzite $AgInS_2$ which contains 32 atoms, including 8 silver atoms, 8 indium atoms and 16 sulfur atoms. The relaxed lattice constants of wurtzite $AgInS_2$ are a = 7.041 Å, b = 8.196 Å and c = 6.574 Å, which are consistent with the experiment results of a = 6.977 Å, b = 8.273 Å and c = 6.695 Å [23]. The relaxed supercell of pure wurtzite $AgInS_2$ is shown in Fig. 1(a), and the vacancy defect models of wurtzite $AgInS_2$ supercell are shown in Fig. 1(b) and (c), respectively. The supercells of wurtzite $AgInS_2$ with the silver and indium atoms replaced by tin atoms are relaxed as shown in Fig. 1(d) and (e), respectively.

The band structure and density of state (DOS) of wurtzite $AgInS_2$

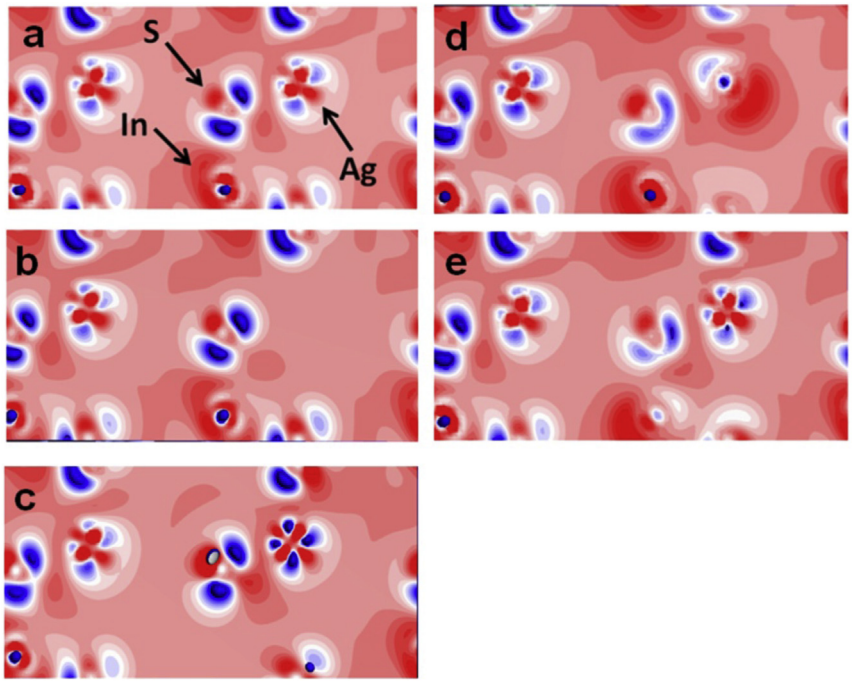

Fig. 4. Electron density of wurtzite $AgInS_2$ with different structural defects. (a) Electron density of pure wurtzite $AgInS_2$; (b) Electron density of wurtzite $AgInS_2$ with silver vacancy; (c) Electron density of wurtzite $AgInS_2$ with indium vacancy; (d) Electron density of wurtzite $AgInS_2$ a silver atom of which is replaced by a tin atom; (e) Electron density of wurtzite $AgInS_2$ an indium atom of which is replaced by a tin atom.

with vacancy defects and tin doping along the high symmetry directions in the Brillouin zone are calculated based on the PBE, and the results are shown in Figs. 2 and 3, respectively. Fig. 2(a) shows the band structure model of pure wurtzite $AgInS_2$, and the Fermi level indicated by a blue line is set to zero. Both the valence band maximum and the conduction band minimum of wurtzite $AgInS_2$ are in G line, showing that wurtzite $AgInS_2$ is a direct band gap semiconductor, and the density of states (DOS) shown in Fig. 3(a) indicate that the top of valence band (from −2 to 0 eV) mainly includes an antibonding state of Ag-d and S-p, and the bottom of conduction band (from 0 to 2 eV) mainly consists of antibonding state of In-s, S-s. Therefore, it can be concluded that the valence band maximum is mainly determined by the interaction of silver atom and sulfur atom, and the conduction band minimum is mainly determined by the interaction of indium atom and sulfur atom. The definition of semiconductor type indicates that the optical band gap from the Fermi level to the bottom of conduction band is a characteristic of P-type semiconductor and the band gap from the top of valence band to the Fermi level is a characteristic of n-type semiconductor. Therefore, $AgInS_2$ shows a characteristic of p-type semiconductor. The simulated band gap is 0.75 eV, which is similar to that of the results reported by the literature [22,23]. It is still less than the experiment value (1.8–2.0 eV) due to the adopted simulated method underestimate the results, but it doesn't affect the profile of band structure. Fig. 2(b) and (c) show the band structure of wurtzite $AgInS_2$ with silver and indium vacancy defects,

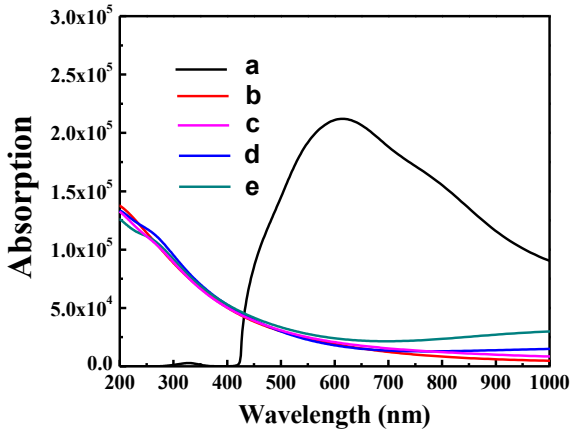

Fig. 5. Calculated optical absorption coefficient of wurtzite $AgInS_2$ with different structural defects. (a) Calculated optical absorption coefficient of pure wurtzite $AgInS_2$; (b) Calculated optical absorption coefficient of wurtzite $AgInS_2$ with silver vacancy; (c) Calculated optical absorption coefficient of wurtzite $AgInS_2$ with indium vacancy; (d) Calculated optical absorption coefficient of wurtzite $AgInS_2$ a silver atom of which is replaced by a tin atom; (e) Calculated optical absorption coefficient of wurtzite $AgInS_2$ an indium atom of which is replaced by a tin atom.

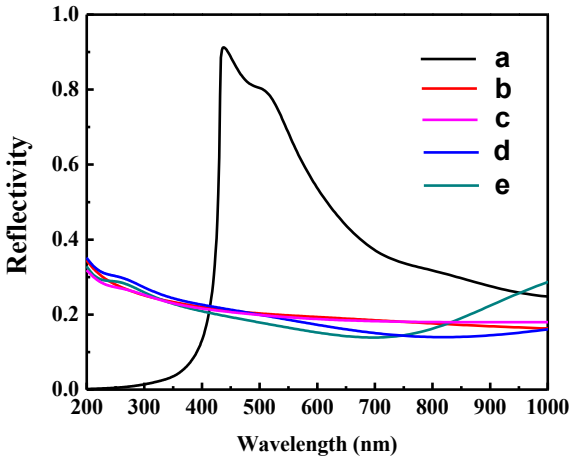

Fig. 6. Reflectivity of wurtzite $AgInS_2$ with different structural defects. (a) Reflectivity of pure wurtzite $AgInS_2$; (b) Reflectivity of wurtzite $AgInS_2$ with silver vacancy; (c) Reflectivity of wurtzite $AgInS_2$ with indium vacancy; (d) Reflectivity of wurtzite $AgInS_2$ a silver atom of which is replaced by a tin atom; (e) Reflectivity of wurtzite $AgInS_2$ an indium atom of which is replaced by a tin atom.

respectively. And the results show that the vacancy defects lead to the introduction of impurity levels, which can narrow the bandgap significantly, and from the PDOS (Fig. 3b and c) of them it can be seen that the S-p orbital which consists in the conduction band is the impurity level. Fig. 2(d) and (e) show the band gap profile of wurtzite $AgInS_2$ with tin doping of silver and indium, respectively; and the impurity levels bend across the Fermi level, which shows a characteristic of metal. It can be seen from the PDOS of Fig. 3(d) and (e) that the impurity levels are Sn-s and S-p orbitals, respectively. Therefore, the calculation results show that vacancy defects can lead to the narrow of the bandgap, and the introduction of tin can enhance the electroconductivity of $AgInS_2$.

Charge density difference can describe the change of electron density distribution which is touched off by the combination of atomic orbital before and after the formation of chemical bonds, and it can indicate the state of the electron transfer process of a chemical bond formation. Charge density difference can be calculated by the formula as follows:

$$\Delta\rho = \rho_{total} - \sum_i \rho_i$$

where ρ_{total} is the total distribution of electron density and ρ_i is the sublattice electron density distribution of each atom.

Fig. 4 shows the distribution of charge density difference (2D model) for $AgInS_2$ with vacancy defects and tin doping at (010) plane. Blue (in web version) indicates electron-missing, and red (in web version) indicates electron enrichment. Fig. 4(a) shows the charge density difference distribution of pure wurtzite $AgInS_2$. It can be seen clearly that the charge density difference distribution of silver atom, indium atom and sulfur atom. Fig. 4(b) shows the charge density difference distribution of silver vacancy defects. We can see clearly the vacancy of silver, and the improvement of charge distribution of sulfide. Obviously, the charge distribution of sulfide is smaller than that of Fig. 4(a) due to the silver vacancy, and the reason is that the sulfide ion is polarized by the other bonding silver atom the electronegative of which is 1.93. But when it is indium vacancy (Fig. 4c), the charge distribution moves to the nearest silver atom at (010) plane due to its strong polarization force. Fig. 4(d) shows the charge density difference distribution of $AgInS_2$ a silver atom of which is replaced by a tin atom. Compared with Fig. 4(a), the charges of sulfur atom move to the vicinity of tin atom due to the electronegativity of the nearest tin atom (1.96) is more greater than that of indium atom (1.78). Fig. 4(e) shows the charge density difference distribution of $AgInS_2$ an indium atom of which is replaced by a tin atom. It can be seen that the charges distribution of sulfur atom changes to smaller than that of Fig. 4(a) due to the electronegativity of the bonding silver atom is almost the same as that of tin atom in the same plane, and the charges move to the vicinity of the other bonded silver atom at another plane. The study results of charge density difference distribution indicates that the electron distribution is significant improved due to the existence of the different vacancy defects and tin doping.

In order to obtain the detailed optical property, the optical absorption coefficient and the reflectivity of wurtzite $AgInS_2$ with vacancy defects and tin doping are calculated as shown in Figs. 5 and 6, respectively. It can be seen that all the absorption curves and reflectivity curves of wurtzite $AgInS_2$ with vacancy defects and tin doping are blue shift. From Fig. 5(a), it can be seen that the wide optical absorption peak of $AgInS_2$ reaches the maximum at about the range of 550–650 nm (about 2.2×10^5). The curve declines sharply at the range of 420–550 nm, and the result is consistent with the reflectivity curve of Fig. 6(a), the maximum sharp peak of which is at the same range, indicating that the maximum value of reflectivity is corresponding to the minimum value of absorption. The absorption curves of wurtzite $AgInS_2$ with vacancy defects and tin doping are shown in Fig. 5(b)–(e), respectively; compared with pure wurtzite $AgInS_2$, all the absorption curves are blue shift, indicating that impurity levels improve the performance of light absorption. It can be seen that the absorption of wurtzite $AgInS_2$ with vacancy defects (Fig. 5b and c) are less than that of wurtzite $AgInS_2$ with tin doping (Fig. 5d and e) in the visible region, but the reflectivity of wurtzite $AgInS_2$ with vacancy defects (Fig. 6b and c) are greater than that of wurtzite $AgInS_2$ with tin doping (Fig. 6d and e) in the visible region, the results of which indicate the complementary relation of absorption and reflectivity, and it also shows the validity of the simulated results.

4. Conclusions

The supercells of wurtzite $AgInS_2$ with vacancy defects and tin doping are set up and the electronic structure and optical property of them have been investigated by the first principle. The results show that $AgInS_2$ is a direct band gap semiconductor, and it shows different property when different defects is existent in the supercell of wurtzite $AgInS_2$. The electroconductivity is improved when a metal atom of the supercell of $AgInS_2$ is replaced by a tin atom. The optical property study shows that the absorption spectrum and reflectivity of $AgInS_2$ are improved after the metal atoms are replaced by the tin atoms.

Acknowledgement

This paper is supported by the Gansu Provincial Youth Science and Technology Fund Projects (1506RJYA093), National Natural Science Foundation of China (grant No. 51402142), the Doctoral Fund of Lanzhou university of technology (01-061402), the China Postdoctoral Science Foundation (2015M572615), the Program for Hongliu Young Teachers in Lanzhou University of Technology (Q201401) and the National Natural Science Foundation of China (No. 21301084).

References

[1] E. Baeissa, J. Ind. Eng. Chem. 20 (2014) 3270.
[2] J. Yin, J. Jia, G. Yi, Mater. Lett. 111 (2013) 85.
[3] W. Xiang, C. Xie, J. Wang, J. Zhong, X. Liang, H. Yang, L. Luo, Z. Chen, J. Alloys Compd. 588 (2014) 114.
[4] A. Tadjarodi, A.H. Cheshmekhavar, M. Imani, Appl. Surf. Sci. 263 (2012) 449.
[5] C.H. Wang, K.W. Cheng, Ch. J. Tseng, Sol. Energy Mater. Sol. Cells 95 (2011) 453.
[6] L. Tan, S. Liu, X. Li, I.S. Chronakis, Y. Shen, Colloids Surf. B Biointerfaces 125 (2015) 222.
[7] M. Anantha Sunil, K.G. Deepa, J. Nagaraju, Thin Solid Film 550 (2014) 71.
[8] Q. Cheng, X. Peng, C.K. Chan, ChemSusChem 6 (2013) 102.
[9] M.L. Albor Aguilera, J.R. Aguilar Hernández, M.A. González Trujillo, M. Ortega Lopez, Sol. Energy Mater. Sol. Cells 91 (2007) 1483.
[10] M.L. Albor-Aguilera, D. Ramírez-Rosales, M.A. González-Trujillo, Thin Solid Film 517 (2009) 2535.
[11] C. Li, Y.F. Zhao, Y.Y. Gong, T. Wang, C.Q. Sun, Phys. Chem. Chem. Phys. 16 (2014) 21446.
[12] Y. He, G. Galli, Chem. Mater. 26 (2014) 5394.
[13] V. Kumar, S.K. Tripathy, J. Alloys Compd. 582 (2014) 101.
[14] M.R. Benam, N. Abdoshahi, M.M. Sarmazdeh, Comput. Mater. Sci. 84 (2014) 360.
[15] Y.X. Han, C.L. Yang, Y.T. Sun, M.S. Wang, X.G. Ma, J. Alloys Compd. 585 (2014) 503.
[16] C. Gionco, M.C. Paganini, E. Giamello, R. Burgess, C. Di Valentin, G. Pacchioni, J. Phys. Chem. Lett. 5 (2014) 447.
[17] P. Nath, S. Chowdhury, D. Sanyal, D. Jana, Carbon 73 (2014) 275.
[18] J.A. Dawson, J.A. Miller, I. Tanaka, Chem. Mater. 27 (2015) 901.
[19] C. Chen, J. Zhang, B. Zhang, H.M. Duan, J. Phys. Chem. C 117 (2013) 4337.
[20] S. Caliskan, S. Guner, J. Alloys Compd. 619 (2015) 91.
[21] J. Li, H. Yuan, Z. Zhu, J. Alloys Compd. 640 (2015) 290.
[22] D. Huang, C. Person, Chem. Phys. Lett. 591 (2014) 189.
[23] J. Liu, S. Chen, Q. Liu, Y. Zhu, Y. Lu, Comput. Mater. 91 (2014) 159.